NANOSTRUCTURED MESOPOROUS TiO_2 DOPED WITH CeO_2 AND ZrO_2 OBTAINED BY UREA ASSISTED HOMOGENEOUS HYDROLYSES METHOD AS CATALYSTS FOR HYDROGEN PRODUCTION

Aleksandra A.Mileva[1]*, Gloria S. Issa[1], Jiří Henych[2], Tanya S. Tsoncheva[1]

[1]Institute of Organic Chemistry with Centre of Phytochemistry, Bulgarian Academy of Sciences, Acad. G. Bontchev str., bl.9, 1113, Sofia, Bulgaria

[2] Institute of Inorganic Chemistry of Czech Academy of Sciences, 25068, Řež, Czech Republic

Abstract

Mesoporous titanium–zirconium and titanium- cerium oxide materials with different composition (Ce(Zr)=25, 50 and 80 mol %) were prepared by homogeneous precipitation with urea and further calcination at 773 K. The obtained materials were characterized by low temperature nitrogen physisorption, XRD, UV–Vis, FTIR and Raman spectroscopy. Their catalytic activity was tested in methanol decomposition to CO and hydrogen with a potential application as alternative fuel. All binary oxides possess higher specific surface area and higher dispersion as compared to the individual oxides. For the Ti-Zr binary materials the BET surface area passed through a maximum for the sample with equimolar Zr/Ti ratio, while it permanently increased with the decreased of Ce content in Ti-Ce samples. The Raman and XRD data indicated significant structure and morphology changes with the variation of Ce and Zr content due to the formation of mixed oxides. The catalytic behavior of the binary materials in methanol decomposition was in a complex relation with the improved textural characteristics of binary materials and to the specific interaction between the individual oxides, which could be successfully controlled by their composition.

Keywords: *nanostructured TiO_2-ZrO_2, nanostructured TiO_2-CeO_2, methanol decomposition*

1. INTRODUCTION

It is known that the hydrogen is the most efficient and environmental energy carriers. Hydrogen has the superior gravimetric energy storage density (120 MJ kg^{-1}) without any harmful emissions upon the conversion of hydrogen energy to electrical energy [1]. However, due to the limitation of the hydrogen storage technologies, its wide use, especially in internal combustion engines, is limited. Recently, the tendency for the use of various compounds (water, hydrocarbons, alcohols, etc.) as a "reservoir" of hydrogen that can be easily stored, transported and release hydrogen in case of need is permanently increases. Methanol is one of the most preferred hydrogen storage compounds, because it can be easy produced by well-established technologies, including from alternative raw materials, as CO_2, biomass or any waste that can be converted into synthes gas [2]. Catalytic decomposition of methanol provides an opportunity for the production of hydrogen-rich gas. An important step in controlling of the decomposition process is the development of highly efficient and inexpensive catalysts to ensure the processes of high activity and stability over a wide temperature range with high selectivity for the desired product. Recently, the transition metal/metal oxide catalysts in nanoscale gain a considerable interest [3]. Among the numerous catalysts, titanium dioxide (TiO_2) has attracted greatest interest due to its high photocatalytic capacity, non-toxicity and cost effectiveness [4]. A lot of data in the literature have demonstrated that catalytic activity of TiO_2 materials could be increased by the introduction of various additives due to the improved dispersion and redox properties of the mixed nanocomposites [5]. The aim of current investigation is to obtain series of nanostructured mesoporous Ti-Ce and Ti-Zr oxides with different composition using urea assisted homogeneous hydrolyses method. The obtained materials were characterized by low temperature nitrogen physisorption, XRD, FTIR UV–Vis, Raman-spectroscopies. The catalytic behaviour in methanol decomposition as a source of syngas was discussed.

2. MATERIALS AND METHODS

2.1. Materials

The pure TiO_2 and CeO_2 and their composites denoted as xTiyCe were prepared by the modified homogeneous hydrolysis of the metal salts with urea as the precipitating agent [6]. Appropriate amount of $TiOSO_4$ (30 g for pure TiO_2) was dissolved in 2L of hot water acidified with H_2SO_4. Then 100 mL of NH_4OH solution was continuously added to the solution while vigorously stirred. The formed white precipitate was washed with water several times to remove sulphate ions and subsequently dissolved by addition of 30 ml nitric acid. Then, a corresponding amount of $Ce(NO_3)_3.6H_2O$ was dissolved in the solution (Ti:Ce molar ratios 1:0, 8:2, 1:1, 2:8, 0:1). This mixture was diluted to a final volume (4 L), and 200 g of urea was added. Heating of the solution at 85 °C for 6 hours leads to a formation of the precipitate. After washing with water by decantation, yellowish powder was filtered, dried, and annealed at 500 °C. Alternatively, the Zr^{4+} doped nanocrystalline titania samples, denoted as xTiyZr, were prepared by homogeneous hydrolysis of $TiOSO_4$ and $ZrOSO_4$ using urea as the precipitation agent. Typically, 100g $TiOSO_4$ were dissolved in 100 ml hot distilled water acidified with 98% H_2SO_4. After dilution into 4 L of distilled water, defined amount of $ZrOSO_4$ and 400g of urea were added. The mixture was heated to 373K under stirring and kept at this temperature for 9h until pH 7 was reached and ammonia escaped from the solution. The formed precipitates were washed by distilled water with decantation, filtered, dried at temperature 378K in a dry oven and calcined up to 773K (/min) for 2h at the final temperature.

2.2. Methods

The textural characteristics were collected from nitrogen adsorption-desorption isotherms measured at 77 K using a Quantachrome NOVA 1200 apparatus. Powder X-ray diffraction patterns were collected on a Bruker D8 Advance diffractometer with Cu Kα radiation using a LynxEye detector. The UV–Vis spectra were recorded on a Jasco V-650 UV-Vis spectrophotometer equipped with a diffuse reflectance unit. FTIR spectra were recorded on a Bruker Vector 22 spectrometer at a resolution of 1–2 cm^{-1}, accumulating 64–128 scans using KBr pellets technique. Raman spectra were acquired with a DXR Raman microscope using a 780 nm laser.

2.2.1. Methanol decomposition

Methanol conversion was carried out under temperature-programmed regime within the range of 350–770K with heating rate of 1Kmin^{-1} in a flow of 1.57kPa methanol in argon. On-line gas chromatographic analyses were performed on a HP 5890 apparatus equipped with flame ionization detector and detector of thermo-conductivity on a PLOT Q column, using an absolute calibration method and a carbon-based material balance.

3. RESULTS AND DISCUSSION

In Figure 1 are presented nitrogen physisorption isotherms for the obtained xTiyCe and xTiyZr samples and the corresponding data are listed in Table 1. According to IUPAC classification the isotherms of all materials are of type IV, typical of materials with mesoporous structure. With the decrease of Ce content in the bi-component Ti-Ce samples, increase of the BET surface area and total pore volume were observed. For the Ti-Zr binary materials the BET surface area changed via maximum for the sample with equimolar Ti/Zr ratio (Table 1). The texture parameters of all binary oxides overcame the expected ones if the samples were considered as a mechanical mixture of the individual oxides. This could be due to the improvement in the dispersion and/or interaction between the components. Note that urea assisted homogeneous hydrolyses method was less successful for the preparation of pure mesoporous ZrO_2.

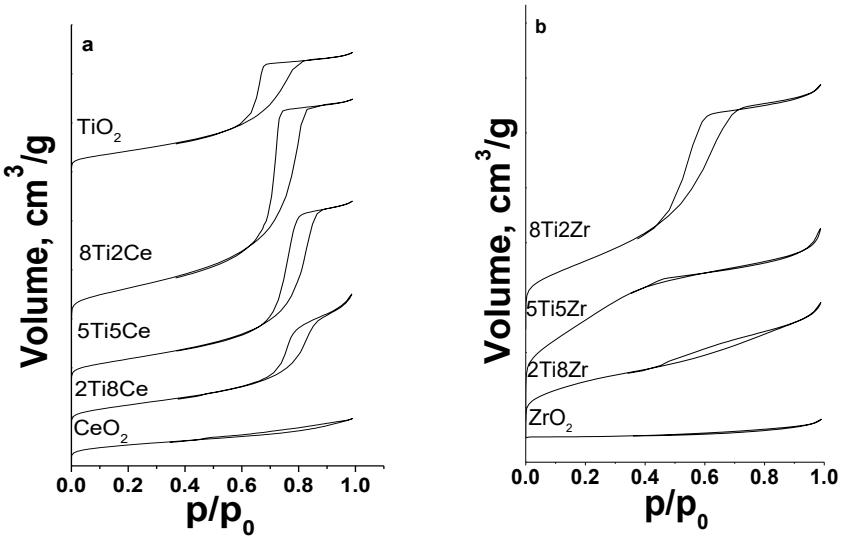


Figure 1. Nitrogen physisorption isotherms of Ti-Ce (a) and Ti-Zr(b) materials.

Table 1. Nitrogen physisorption data of mono- and bi-component TiCe and TiZr materials

Sample	**BET, $m2g^{-1}$**	**Pore Volume, mlg^{-1}**
TiO_2	97	0.19
8Ti2Ce	146	0.36
5Ti5Ce	117	0.30
2Ti8Ce	107	0.21
CeO_2	76	0.07
8Ti2Zr	137	0.21
5Ti5Zr	204	0.16
2Ti8Zr	112	0.11
ZrO_2	2	0.02

The XRD patterns of Ti-Ce and Ti-Zr samples are shown in Figure 2a and Figure 2b, respectively. The data for the phase composition, unit cell parameters and average crystallite size are listed in Table 2. The XRD pattern of pure titania showed typical diffraction peaks of anatase phase (25.5°, 37.9°,47.8°, 53.6°, 54.8°, 62.6° and 74.9°) with average crystallite size of about 13 nm [8]. Diffraction peaks typical of face centered cubic fluorite phase with average crystallite size of about 13 nm are observed for the mono-component ceria [9]. The XRD patterns of pure ZrO_2 consist of reflections characteristic for tetragonal ZrO_2 phase with average crystallite size of about 30 nm. The observed reflections were broader for binary materials as compared to individual oxides, which evidenced higher dispersion of the particles. In the samples with higher Zr content, the appearance of a plateau, is due to formation of very finely dispersed oxides, which is in consistent with the observed nitrogen physisorption data (Table 1). In the case of 8Ti2Zr sample, slight increase in the unit cell parameters was observed, which could be due to partial incorporation of larger Zr^{4+} ions into the TiO_2 lattice [10]. Just the opposite, the

observed slight decrease of unit cell parameters for the ceria component in binary materialss compared to the individual CeO_2 sample does not exclude substitution of Ce^{4+} ions by smaller Ti^{4+} ions [11].

Table 2. Phase composition, unit cell parameters and average crystallite size for various samples.

Sample	Space Group	Unit cell parameters, Å	Particles size, nm
TiO_2	Anatase, syn	3.7855(6)	13 nm
	Tetragonal – Body-centered I41/amd	9.507(2)	
8Ti2Ce	Anatase, syn	3.771(2)	5 nm
	Tetragonal – Body-centered I41/amd	9.492(8)	
	Cerium Oxide	5.40(1)	2nm
	Face-centered cubic Fm-3m		
5Ti5Ce	Anatase, syn	3.770(5)	5 nm
	Tetragonal – Body-centered I41/amd	9.51(2)	
	Cerium Oxide		
	Face-centered cubic Fm-3m	5.401(2)	7nm
2Ti8Ce	Anatase, syn	3.755(2)	5 nm
	Tetragonal – Body-centered I41/amd	9.55(2)	
	Cerium Oxide	5.410(1)	11nm
	Face-centered cubic Fm-3m		
CeO2	Cerium Oxide	5.4144(6)	13nm
	Face-centered cubic Fm-3m		
ZrO_2	ZrO_2 tetragonal	3.6006(2)	30nm
		5.1859(4)	
8Ti2Zr	Anatase	3.8063(7)	14 nm
		9.625(2)	
5Ti5Zr	Anatase + amorphous		
2Ti8Zr	Amorphous		

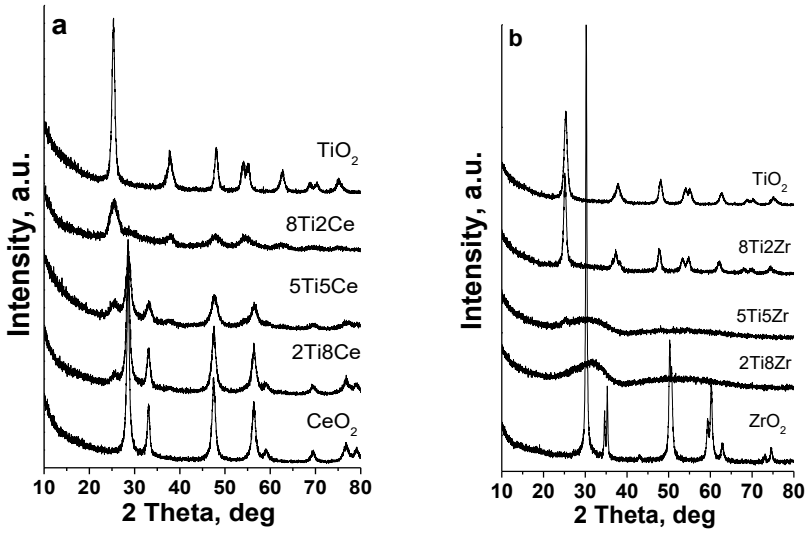


Figure 2. XRD patterns of xTiyCe(a) and xTiyZr(b) materials.

In Fig. 3 are shown the UV–Vis spectra of all Ti-Ce and Ti-Zr materials. The spectrum of pure TiO_2 exhibited absorption edges at 359 nm corresponding to anatase phase [8]. The spectrum of individual CeO_2 consisted of well defined absorption edges in the 300–500 nm range, which is typical of pure ceria phase. The appearance of strong absorbance at about 220 nm in the UV-Vis spectrum of pure ZrO_2 indicated domination of tetragonal ZrO_2 phase [12]. The addition of ceria to titania resulted in "red"shift of the adsorption edge which is slightly influenced by the Ti/Ce ratio. In the spectrum of binary Ti-Zr material, well defined blue shift of the absorption edge was observed and this is most pronounced for 2Ti8Zr. The variation of the absorption edges for the bi-component Ti-Ce and Ti-Zr materials could be assigned to changes in the environment of both metal ions due to the better dispersion of metal oxides and/or to the appearance of strong interaction between them, which is in accordance with the XRD and nitrogen physisorption data (Figure 2, Table 1).

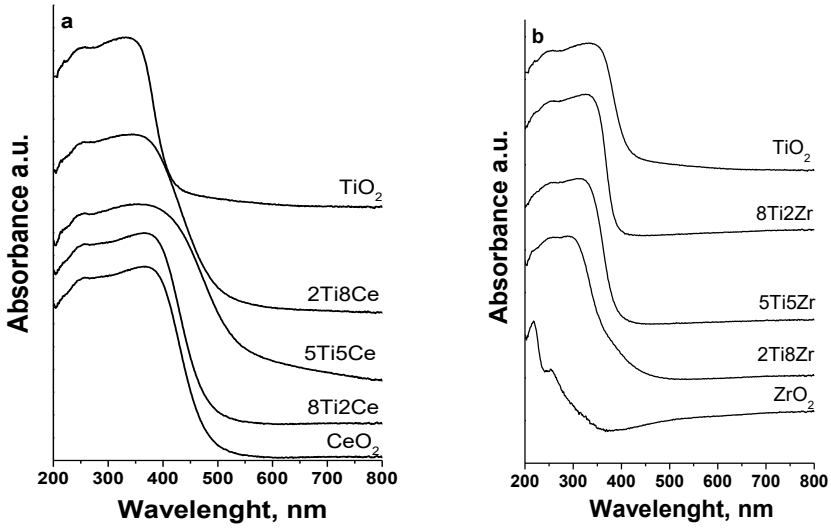


Figure 3. UV-Vis spectra of TiCe (a) and TiZr (b) materials.

Figure 4 shows the FTIR spectra of the obtained TiO_2-CeO_2 and TiO_2-ZrO_2 materials. In the FTIR spectrum of pure TiO_2, absorption band in the 1200–550cm^{-1} region was observed, which could be due to Ti-O and Ti-O-Ti stretching vibrations [13]. The observed absorption band was broader and slightly shifted to higher wavenumbers for all binary materials. These is assigned to lower dispersion of the particles or to the changes in the M-O-M linkages, wchich is in consistent with XRD and UV-Vis data (Table 2, Figure 3). The broad absorption band below 700 cm^{-1} and the absorption in the 700–450 cm^{-1} region observed for the pure CeO_2 and ZrO_2 samples is related to the Ce–O streching vibrations and the presence of tetragonal ZrO_2, respectively.

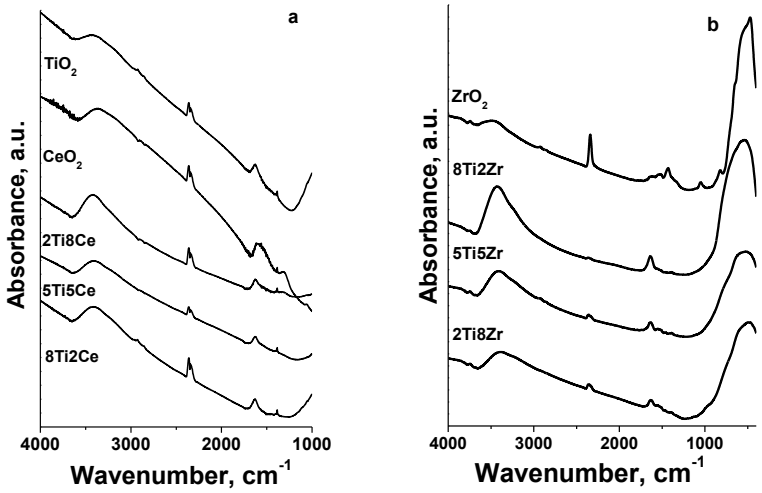


Figure 4. FTIR spectra of TiCe (a) and TiZr (b) materials.

Raman spectra of Ti-Ce and Ti-Zr materials, are presented in Fig.5a and 5b, respectively. The Raman shifts at about 141, 198, 398, 515 and 644 cm^{-1} in the spectra of pure TiO_2 are typical of anatase phase [14]. For the monocomponent ceria sample only one Raman-active E_{2g} mode, centered at about 463 cm^{-1}, was observed, which is typical of cubic fluorite structure [15]. The bands at 142, 270, 317, 458 and 643 cm^{-1} in the ZrO_2 spectrum is assigned to tetragonal ZrO_2 [16]. In the spectra of mixed titania-ceria oxides the intensity of the main peak of ceria significantly decreased. In accordance with the XRD and UV-Vis data this could be assigned to the improved metal oxide dispersion and formation of mixed oxide phases due to the incorporation of Ti^{4+} ions into the ceria lattice. The Raman spectra of the sample with small amount of zirconia (8Ti2Zr) consists of Raman shifts typical of anatase. The observed slight shift of the main band in comparison with pure TiO_2, could be due to the formation of larger anatase particles, which is in consisten with the XRD data. In the spectra of the samples with higher zirconia content (5Ti5Zr, 2Ti8Zr) low intensive Raman shifts were observed, which is assigned to loss of crystallinity. This is probably due to the formation of highly amorphous $Zr_xTi_{1-x}O_4$ solid solution [17].

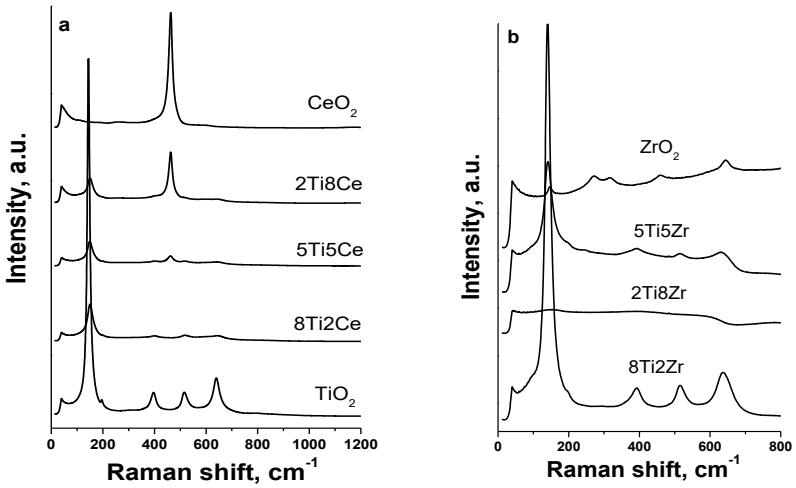


Figure 5. Raman spectra of the individual and mixed TiCe (a) and TiZr (b) materials.

In Figure 6 are presented the temperature dependencies of methanol decomposition on various materials. For both series of the samples methanol decomposition was initiated above 500-550 K. The selectivity to CO, which well illustrates the ability of catalysts to release hydrogen from methanol, is presented in Fig.7. CO_2, CH_4, dimethyl ether (DME) and C_2H_4 were registered as by-products. Among the mono-component materials, CeO_2 demonstrated the highest catalytic activity and selectivity in methanol decomposition to syngas. In contrast, ZrO_2 possessed the lowest catalytic activity but relatively good selectivity to the main products. The observed complex course of the conversion curves for TiO_2 and CeO_2 with the temperature increase was indication for deactivation, most probably due to the formation of non-desorbable products. This tendency disappeared after doping of TiO_2 with CeO_2. However, these binary materials exhibited lower catalytic activity at relatively low temperature despite the improvement of their textural characteristics (Table 1). The significant jump in the conversion curves of TiCe samples above 650 K indicated good stability in the catalytic activity. Just the opposite, TiO_2 dopping with ZrO_2 trended to increase in the catalytic activity, but this effect is strongly affected by the samples composition. The increase in the catalytic activity, combined with preservation of relatively low selectivity to CO for 5Zr5Ti and 2Zr8Ti well correlated with the improved BET surface area. Moreover, the conversion curves profile of these bianry materials followd the complex course of that one for TiO_2. On the base of XRD and spectroscopic results (see above) we assume that the differences in the catalytic behaviour of ZrTi and CeTi materials reflects in a complex way the changes in the textural, surface and redox properties provoked by the incorporation of Zr^{4+} and Ce^{4+} in TiO_2 lattice. We could speculate that the similarity in the electronegativity and the ion radius of Ti and Zr facilitates formation of solid solution, which improves the dispersion and the texural characteristics of the individual oxides without significant changes in their surface and redox properties. Thus, the controlling factor on the catalytic behaviour of TiZr binary materials seems to be the improvement in the BET surface area, which does not influence significantly the selectivity and deposition of non-desorbable products. Just the opposite, the lower degree of incorporation of Ce^{4+} in TiO_2 due to the significantly larger ion radius provides less pronounced texture changes, especially with the increase of Ce content. However, we can expect that the formation of shared Ce-O-Ti bonds with Ce ions with lower electronegativity significantly change the surface and redox properties of TiO_2, which provides lower, but more stable catalytic activity as compared to the individual oxides.

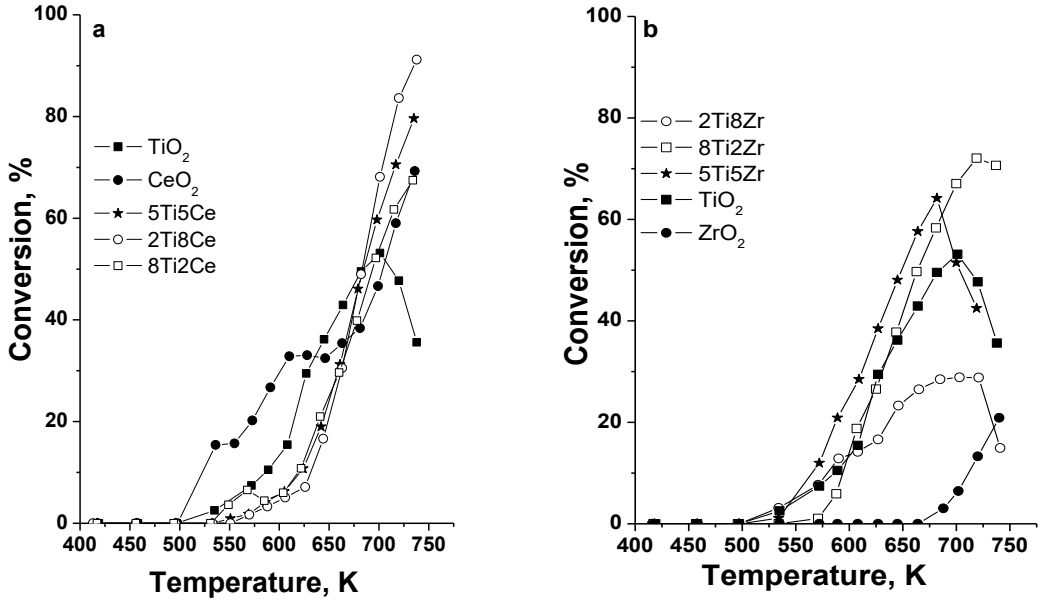


Figure 6. Methanol conversion of TiCe (a) and TiZr (b) materials.

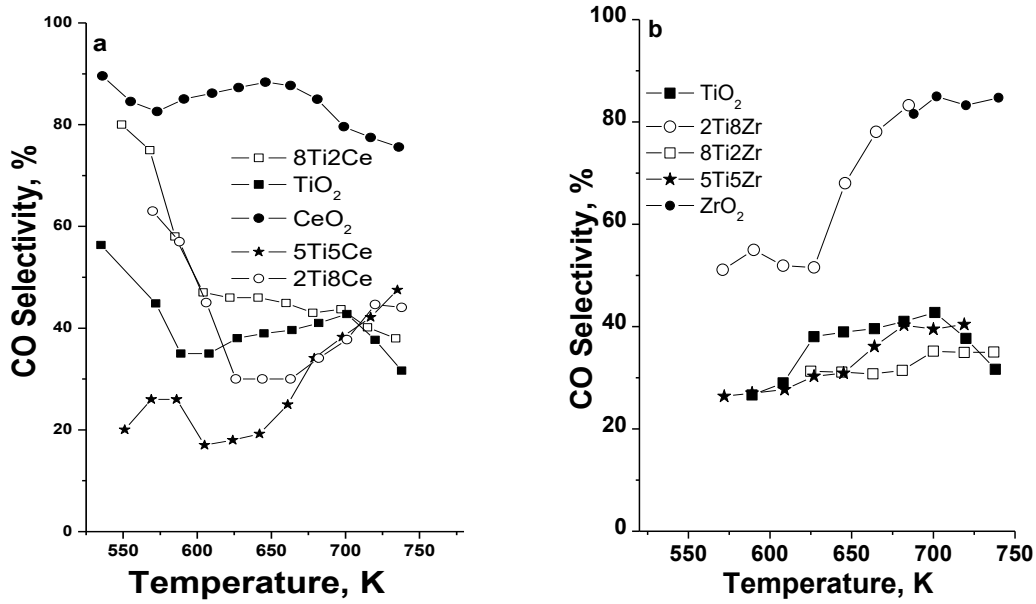


Figure 7. Selectivity to CO of TiCe (a) and TiZr (b) materials.

4. CONCLUSIONS

Homogeneous precipitation with urea were successfully used for the preparation of nanostructured mesoporous TiO_2-CeO_2 and TiO_2-ZrO_2 binary materials in wide range of Ce(Zr)/Ti ratio. All binary materials demonstrate higher dispersion and improved porous characteristics in comparison with their mono-component analogues. The observed specific catalytic behaviour for all mixed oxides is assigned

to the complex relation to the improved textural characteristics and to the specific interaction between the individual oxides, which could be successfully controlled by the sample composition.

ACKNOWLEDGMENTS

Financial support project КП-06-Н-29/2 and bilateral project between Bulgarian Academy of Sciences and Czech Academy of Sciences is gratefully acknowledged. Project BG05M2OP001-1.002-0019:„Clean technologies for sustainable environment – water, waste, energy for circular economy“(Clean&Circle), for development of a Centre of Competence is also acknowledged.

REFERENCES

1. Shi L., Qi S., Qu J., Che T., Yi S., Yang B., 26 February 2019, *Integration of hydrogenation and dehydrogenation based on dibenzyltoluene as liquid organic hydrogen energy carrier*, Volume 44, Issue 11, Pages 5345-5354, International Journal of Hydrogen Energy, School of Chemical Engineering and Technology, Xi'an Jiaotong University, Xi'an, Shaanxi, China
2. Santiago M., Barbera K., Ferreira C., CurullaFerré D., Kolb P., Pérez-Ramírez J., 2012, *By-product co-feeding reveals insights into the role of zinc on methanol synthesis catalysts*, 21, 63, Catal. Communication, Institute for Chemical and Bioengineering, Department of Chemistry and Applied Biosciences, Zurich, Switzerland.
3. Liu H., Yu I., Chen W., Li Y., 2012, *The Progress of TiO_2 Nanocrystals Doped with Rare Earth Ions*, Article ID 235879, doi 10.1155/2012/235879, J. Nanomater., Department of Materials Science and Engineering, Nanchang University, China.
4. Suna S., Zhaoa R., Xiea Y., Liuc Y., June 2019, *Photocatalytic degradation of aflatoxin B1 by activated carbon supported TiO2 catalyst*, Volume 100, Pages 183-188, Food Control., College of Food Science and Technology, Henan University of Technology, Lianhua, China.
5. Schmid G., Baumle M., Greekens M., Heim I., Osemann C., Sawatowski T., 1999, *Current and future applications of nanoclusters*, 28, 179, Chemical Society Reviews.
6. Subrt J., Stengl V., Bakardjieva S., Szatmary L., 2006, *Synthesis of spherical metal oxide particles using homogeneous precipitation of aqueous solutions of metal sulfates with urea*, 169, 33, Powder Technol., Institute of Inorganic Chemistry, Academy of sciences of the Czech Republic, Czech Republic.
7. Stengl V., Bakardjieva S., Murafa N., Oplu F., 2008, *Zirconium Doped Titania: Destruction of Warfare Agents and Photocatalytic Degradation of Orange 2 Dye*, 1, 1-7, The Open Process Chemistry Journal, 1Institute of Inorganic Chemistry AS Czech Republic v.v.i and Military Technical Institute of Protection Brno, Czech Republic.
8. Altomare M., Dozzi M., Chiarello G., Paola A., Palmisano L., Selli E., 2015, *High activity of brookite TiO2 nanoparticles in the photocatalytic abatement of ammonia in water*, 252, 184, Catalysis Today, Dipartimento di Chimica, Università degli Studi di Milano, Italy.
9. Shan W., Liu F., He H., Shi X., Zhang C., 2012, *An environmentally-benign CeO2-TiO2 catalyst for the selective catalytic reduction of NOx with NH3 in simulated diesel exhaust*, 184, 160-165, Catal. Today, Research Center for Eco-Environmental Sciences, Chinese Academy of Sciences, China.
10. Zhang J., Li L., Liu D., Zhang J., Hao Y., Zhang W., 2015, *Multi-layer and open three-dimensionally ordered macroporous TiO_2–ZrO_2 composite: diversified design and the comparison ofmultiple mode photocatalytic performance*, 86, 818-828, Materials & Design, College of Materials Science and Engineering, Qiqihar University, China.

11. Espinosa de los Monteros A., Lafaye G., Cervantes A., Del Angel G., Barbier Jr. J., Torres G., 2015, *Catalytic wet air oxidation of phenol over metal catalyst (Ru, Pt) supported on TiO2–CeO2 oxides*, 258, 564-569, Catalysis Today, Institute of Chemistry of Poitiers: Materials and Natural Resources (IC2MP) UMR 7285 CNRS, Université de Poitiers, France.
12. Basahel S., Ali T., Mokhtar M., Narasimharao K., 2015, *Influence of crystal structure of nanosized ZrO2 on photocatalytic degradation of methyl orange*, 10, 73–86, Nanoscale Res. Lett., Department of Chemistry, Faculty of Science, King Abdulaziz University, Kingdom of Saudi Arabia.
13. Seo K., Hyun Y., Lee C., 2014, *Ultrasonochemical coating and characterization of TiO2-coated zirconia fine particles*, 20, 1819–1824J. Ind. Eng. Chem., Department of Chemistry, Keimyung University, Republic of Korea.
14. Yang S., Zhu W., Jiang Z., Chen Z., Wang J., 2006, *The surface properties and the activities in catalytic wet air oxidation over CeO2–TiO2 catalysts*, 252, 8499, Appl. Surf. Sci., Department of Environmental Science and Engineering, Tsinghua University, China.
15. Ding J., Lin J., Xiao J., Zhang Y., Zhong Q., Zhang S., Guo L., Fan M., 2016, *Effect of fluoride doping for catalytic ozonation of low-temperature denitrification over cerium–titanium catalysts*, 665, 411, J. Alloys Comp., School of Chemical Engineering, Nanjing University of Science and Technology, China.
16. Yung M., Holmgreen E., Ozkan U., 2007, *Cobalt-based catalysts supported on titania and zirconia for the oxidation of nitric oxide to nitrogen dioxide*, 247, 356–367, J. Catal., Department of Chemical and Biomolecular Engineering, The Ohio State University, Columbus, USA.
17. Daturi M., Cremona A., Milella F., Busca G., Vogna E., 1998, *Characterisation of zirconiatitania powders prepared by coprecipitation*, 18, 1079–1087, J. Eur. Ceram. Soc., Istituto di Chimica, Facoltàdi Ingegneria, Universitàdi Genova, Italy.